Improved Methodology for Automated SEM/EDS Non-Metallic Inclusion Analysis of Mini-Mill and Foundry Steels

Marc Harris
Obinna Adaba
Simon Lekakh
Ron O'Malley
Von L. Richards

Missouri University of Science and Technology
Materials Science & Engineering Dept.
1400 N Bishop
Rolla, MO 65409

ABSTRACT

Automated Feature Analysis (AFA) provides the means to rapidly characterize large inclusion populations. System settings must be optimized to properly detect and interpret the important inclusion characteristics. The effects of sample area and AFA parameter settings (step size, magnification and threshold) on inclusion characterization results has been investigated and optimized. Methodologies for determining average inclusion chemistry, total element concentrations within inclusions, and for using joint ternary diagrams with size visualization to represent inclusion populations are presented. These methodologies were applied to samples collected from industrial steel mill and steel foundries and demonstrated in this study.

INTRODUCTION

Non-metallic inclusions are an inevitable consequence of steelmaking and are undesirable for the most part. Mechanical properties are largely affected by them and some inclusions promote clogging of submerged entry nozzles (SEN) [1-4]. Complete removal however is not necessary and cleanliness requirements are determined by various thresholds on inclusion characteristics such as amount, size, composition, and distribution[1,5]. These thresholds vary by grade and requirements are increasingly more stringent. Much research has been conducted on methods of inclusion control to minimize the potentially detrimental effects on final properties and there are a vast number of techniques available for characterization of inclusions[1-12]. There is however, a growing need for a time efficient, effective method of characterizing vast numbers of inclusions for the modern day steel producers.

Automated SEM/EDS provides the means to rapidly characterize large inclusion populations providing information about amount size, composition and distribution of inclusions. With the growing computational power available, post-processing of the vast quantities of data output by such a system has also become more efficient. These devices have become popular among steel mills and have proven to be applicable to steel foundries, although, procedures will differ greatly owing to the large difference in process and cleanliness requirements. Precautions also need to be taken in data collection and analysis. Small polished sections from samples taken during liquid steel processing are analyzed and represent only a small fraction of the melt volume while typically being assumed as representative. In addition, collected liquid steel in the sampler is subject to different cooling rates during solidification that can alter the inclusion characteristics[13-14]. Ruby-Meyer et al [5]showed using CFD Fluent calculations that the last section to solidify in a lollipop sampler is at the center. Ola Ericsson[9] investigated the solidification rate for a 12 mm thick stainless steel lollipop sample and observed that the solidification rate could differ by as much as 10 °C/s. System parameter settings and the methods used to post process the typically large quantity of data obtained in an SEM/EDS scan can also lead to misinterpretations.

A methodology has been developed and presented here for accurate, repeatable inclusion analysis using an automated feature analysis SEM/EDS system. This is based on experiments conducted at the Peaslee Steel Manufacturing Research Center (PSMRC), Missouri University of Science and Technology. The ASPEX Pica 1020 SEM/EDS system was used in this study, the basic functionality of which was examined. Both foundry and mill samples were collected from liquid processing steps with the aim of developing accurate and repeatable methods of in-depth inclusion analysis.

EXPERIMENTAL PROCEDURE

Sample Collection and Preparation

Industrial samples were taken during liquid steel processing using un-killed sampler types in order to prevent non-representative inclusion populations from forming. Steel chilled immersion samplers were chosen for their wide applicability and common use in industry. For this reason both center and surface sections were considered for analysis: representing different cooling rates in the sampler. Figure 1 is a schematic of both section locations in the sampler. Grinding was done using SiC media (180, 400, 600, 1200 grits), polished using 3µm diamond paste, and finished using a 0.1µm diamond paste. Metallographic preparation was done in accordance to ASTM E3-11 for all samples.

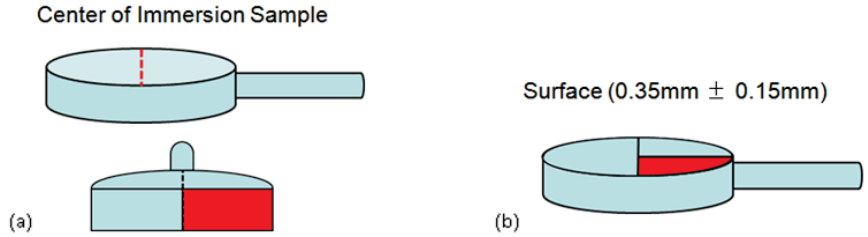

Figure 1. Schematic of immersion samplers with a) center sectioning region highlighted and b) surface sectioned area highlighted (approximately 0.35 mm below surface after sample grinding and polishing).

Automated SEM/EDS Analysis

After preparation, samples were scanned using an automated SEM/EDS system (ASPEX PICA 1020), the simplified procedure of which can be broken down into four steps: 1) SEM location of a feature of high z-contrast; 2) EDS spectrum analysis of the located high z-contrast feature; 3) check of spectrum counts to exclude porosity; 4) recording of all relevant data. Consideration of only a limited number of elements aided in minimizing error in compositional data obtained from EDS spectra. Elements considered included: Mg, Al, Si, Zr, S, Ca, Ti, and Mn. Fe was not considered in the EDS spectra as the interaction volume of the electron beam would affect compositional results in favor of Fe. Scans were performed with varied minimum diameter thresholds, step sizes, and magnification and the effect of these parameters on detection capabilities considered. Approximately 15-30% dead time was used, 20 kV accelerating voltage, and a nominal EDS detection time of 1 second (optimal settings for the instrument and elements of interest). Porosity was excluded from consideration using an EDS count threshold of 1000, an example of which can be seen in Figure 2. A Monte-Carlo simulation of randomly distributed inclusions showed that 500-700 counted inclusions from each specimen is enough to accurately represent the inclusion population. In this study, an average of 2500 inclusions were experimentally counted for improved statistical analysis

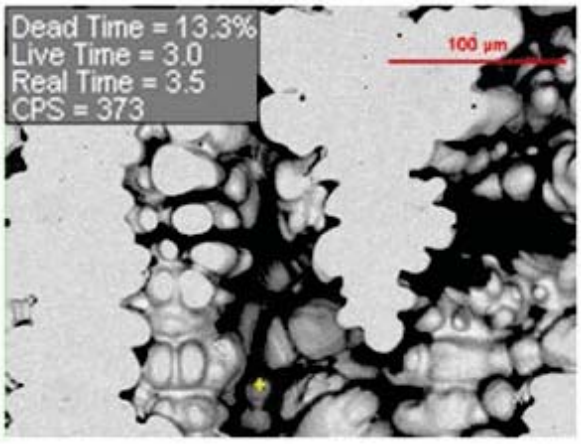

Figure 2. Large region of porosity with low counts per second (CPS) that leads to exclusion from analysis.

RESULTS

ASPEX Settings

Figure 3 is a schematic of how detection and measurement is done using the ASPEX. The electron beam moves in steps (bold black dots) which are determined by the SEM step size setting used. Once a feature is detected a much finer resolution is used (smaller dots) for the measurement of the inclusion. With increasing step size, the possibility of detecting small features

decreases, and as the magnification increases, the separation of the smaller dots decreases thus, increasing the accuracy of measurement. Before the start of an AFA, a minimum diameter threshold is set that determines the minimum size of an inclusion that will be characterized. It is therefore important that the selected step size is less than the minimum diameter threshold setting to detect the maximum number of inclusions.

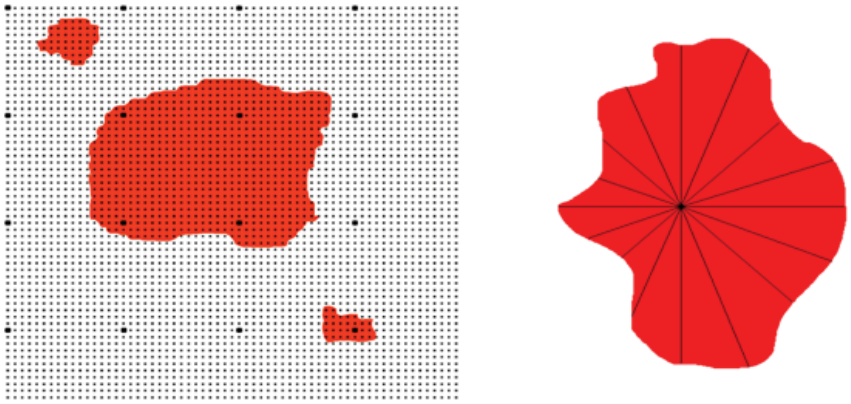

Figure 3. ASPEX feature detection method and area measurement methods.

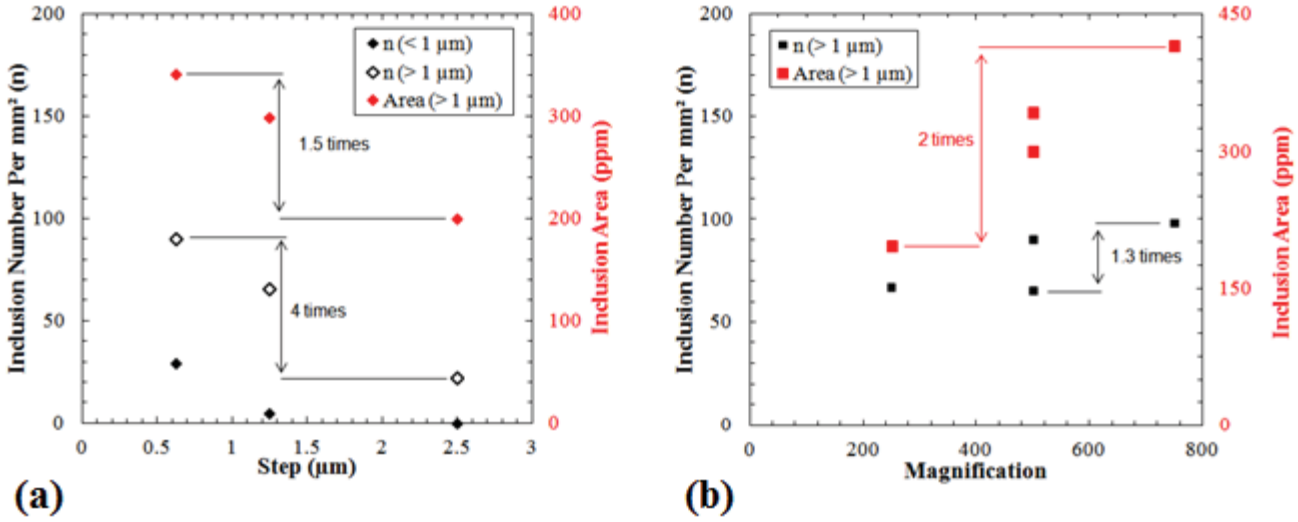

Figure 4. Effect of (a) step size and (b) magnification on number of inclusions detected per area and inclusion area fraction.

Figure 4 shows how the experimentally measured number density and area fraction vary with both step size and magnification for the same analyzed area. The counted values of both number density and area fraction decrease with increasing step size and increase with increasing magnification. Step size was found to have a larger effect on number density while area fraction is affected more by the magnification.

The analyzed area fraction and number of detected inclusions was found to be heavily dependent on the minimum diameter threshold chosen (see Figure 5). The behavior of this curve suggests that a minimum diameter threshold of approximately 0.75 µm should be the largest chosen for an encompassing analysis. As the threshold increases beyond 0.75 µm the resulting area fraction and number of detected inclusions drops significantly, as large numbers of inclusions are going undetected. The variation of the number of detected inclusions below 0.75 µm is reduced but still increases continuously, evidence that there is a population of sub micron (< 0.5 µm) sized inclusions that were not detected. The minimum diameter threshold could not be reduced below 0.5 µm as it was the limit of accurate detection of the instrument; however the area fraction contribution of such small inclusions was determined to be insignificant. Below 0.75 µm in diameter the variation for the resulting area fraction is minimal indicating the true value of the sample area fraction has been obtained since detection of smaller inclusions has no observable effect.

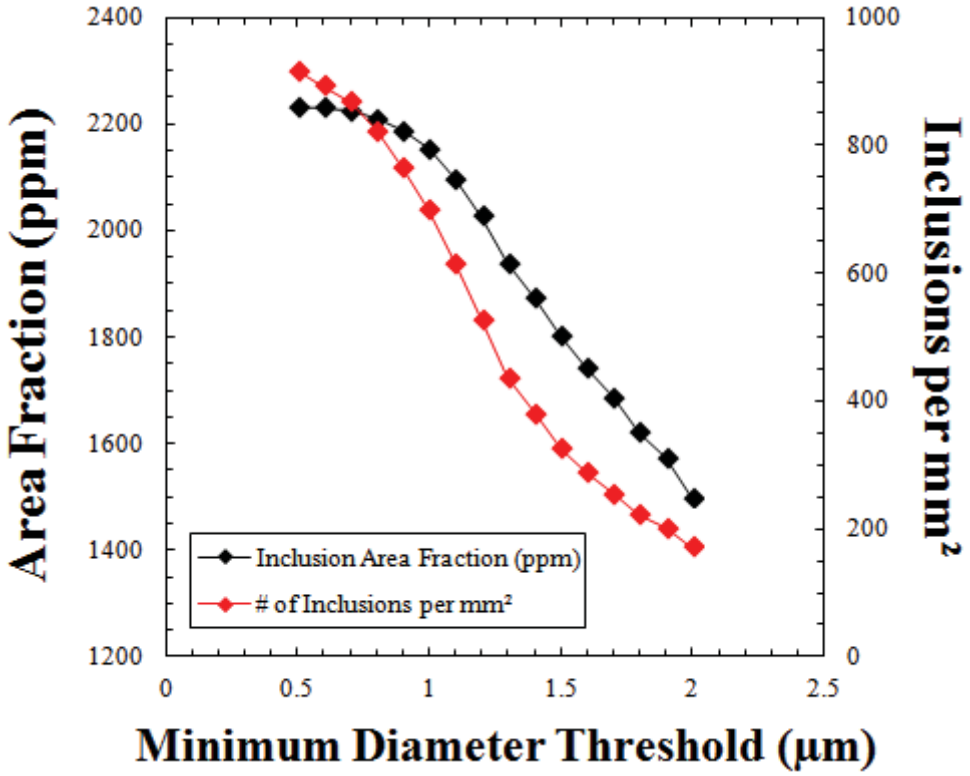

Figure 5. Effect of minimum size setting on reported area fraction and population density.

It was found that scans performed using a 0.5 µm minimum diameter threshold (limit of instrument) were optimal for determining an accurate inclusion area fraction. A search grid step size of 0.16 µm was determined to be more than sufficient for 100% detection of inclusions as small as 0.5 µm in diameter (≤0.35 µm according to Equation 1). The optimal step size is related to the minimum diameter threshold as:

$$s \leq \frac{\sqrt{2}}{2} D_{min} \qquad (1)$$

where: s is the search grid step size, and D_{min} is the minimum diameter threshold. This relationship holds for a square search grid pattern and is based on the worst case scenario of an infinitesimally thin inclusion extending from one corner of the search grid to the other. The result is the maximum step size for 100% detection of inclusions as small as D_{min}.

To further understand the effect of settings on the measured number density and area fraction of inclusions a test was carried out using the SEM calibration standard (Figure 6). The standard is composed of different sized spherical particles and Figure 7 shows the change in measured aspect ratio and size of the detected features for different magnifications. It can be seen that as the magnification increases the measured aspect ratio decreases and the diameters approach the actual values (1, 2, 3..10 µm). Additionally, the variation in both aspect ratio and the diameter from the known value decreases. This is due to increased accuracy of measurement, as a larger pixel density from high magnification gives more accurate measures of area, diameter, and aspect ratio.

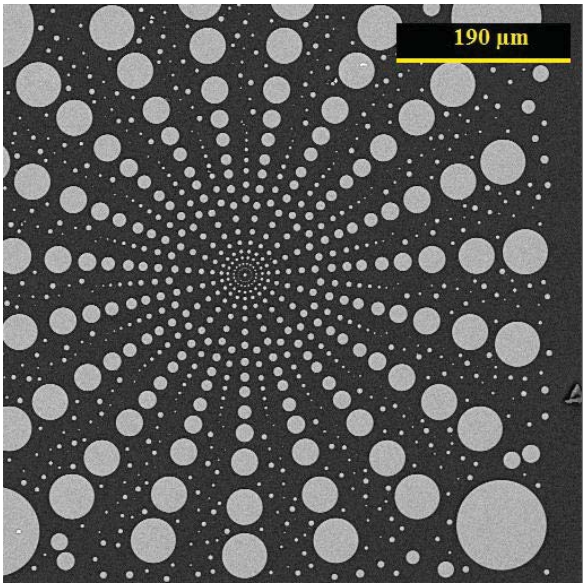

Figure 6. SEM image of calibration standard with known size distribution and aspect ratio of 1.

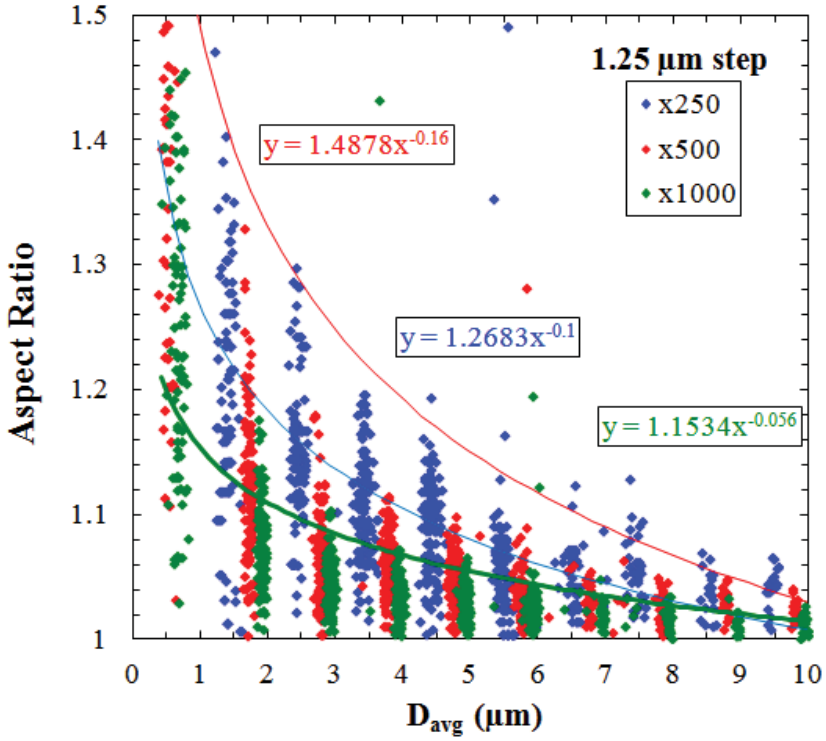

Figure 7. Effect of magnification on the measured particle size and aspect ratio.

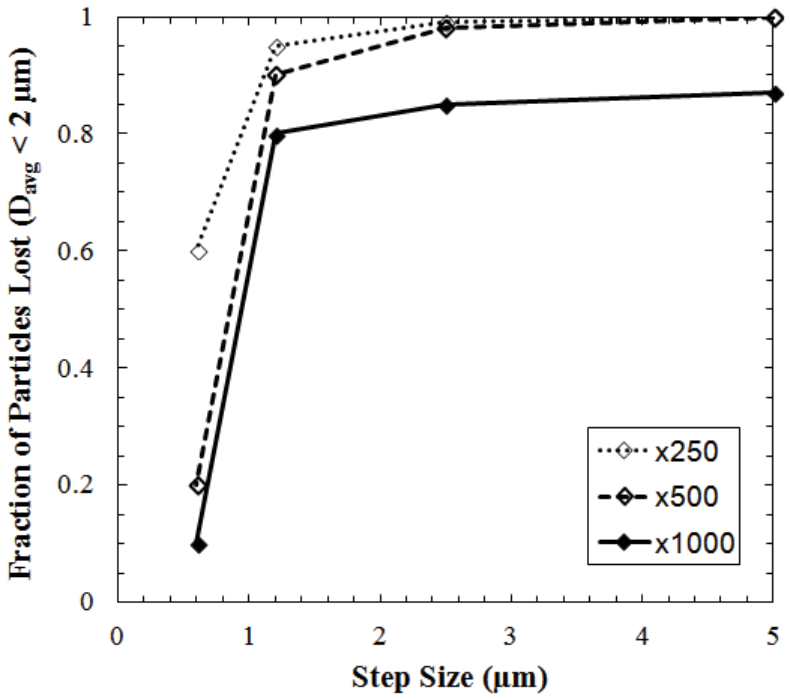

Figure 8. Fraction of undetected small particles below 2 µm diameter for varied step sizes and magnification where 0 denotes no missed particles and 1 denotes total loss.

A quantitative example of the effect of step size and magnification on the fraction of detected particles can be seen most prominently in Figure 8. For small sized inclusions the larger step sizes result in no detection (>80% loss), and for magnifications that are too low the same occurs (differences of 20-50% in detection).

Mass Balance Calculations

A method of calculating a mass balance from SEM-EDS data was developed that allows the study of elemental content contained within inclusions. The areal average elemental composition of inclusions is calculated for each element as follows:

$$\%m = \frac{\sum(\%x)(A_{inclusion})}{A_{total}} \qquad (2)$$

where: *%m* is the areal average mass percent of a given element, *%x* is the amount of respective element in an individual inclusion, $A_{inclusion}$ is the area of the individual inclusion, and A_{total} is the total area of all measured inclusions. The mass balance calculation was performed using the compositional data obtained from the SEM-EDS inclusion analysis and Equation 3:

$$M_{ppm} = \frac{\%m\, A_f\, \rho_i\, w_i}{100\rho_m} \qquad (3)$$

where: M_{ppm} is the mass fraction in ppm of a given element in a sample contained within inclusions, *%m* is the areal average mass percent of a given element, A_f is the total inclusion area fraction, ρ_i is the density of the inclusion associated with the given element, ρ_m is the density of the matrix (taken to be iron), and w_i is the mass fraction of the given element in the associated inclusion compound.

The results of these mass balance calculations were extended to calculate the approximate amount of total oxygen in the samples through the assumption of most-stable compound. This was done as a means to meter the accuracy of the mass balance calculations as oxygen is a low solubility element in iron, almost entirely present in the steel in the form of oxide inclusions. In order to calculate the oxygen content, sulfides were filtered via a sulfur threshold and the remaining inclusions assumed to be stable oxides with the appropriate stoichiometry. The accuracy of varied sulfide thresholds on the total oxygen calculation was compared to an inert gas fusion analysis of total oxygen (see Figure 9). A 30% threshold of sulfur was found to be in closest agreement with the inert gas fusion analysis results. A direct comparison of total oxygen is shown in Figure 10 as a function of process time for two industrial trials. The accuracy of the calculated results is close or inside the 95% confidence interval for most of the inert gas fusion analysis method results and is consistent enough to represent the same trends, indicating the mass balance results are reasonable. Additionally the calculated results are largely within less than 50 ppm of the reported inert gas fusion results with few exceptions.

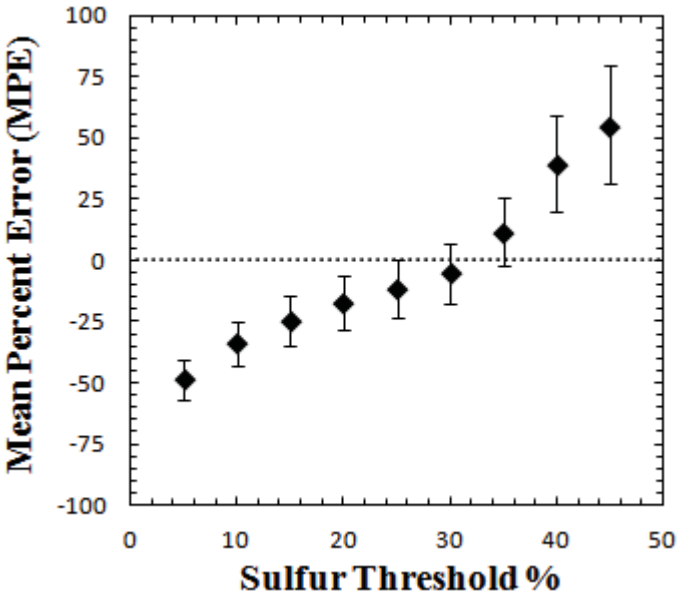

Figure 9. Mean percent error of calculated total oxygen from SEM/EDS data compared to inert gas fusion method versus sulfur threshold used in analysis.

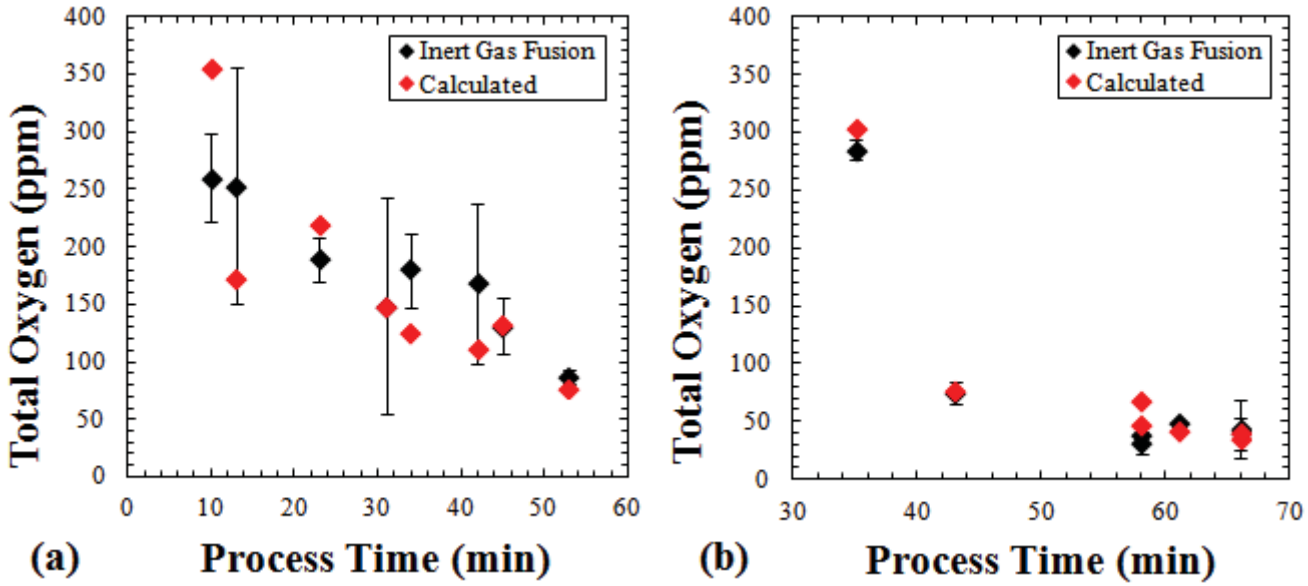

Figure 10. Total oxygen content measured by two methods (calculated with a 30% sulfur threshold and inert gas fusion) in samples taken throughout liquid processing at a) Foundry A and b) Foundry B.

The optimal sulfur threshold was applied in a mass balance calculation of manganese rich inclusions and the results can be seen in Figure 11 for both unfiltered and only oxide inclusions. This method allows examination of mass quantities associated with specific inclusion populations, in this case manganese oxide.

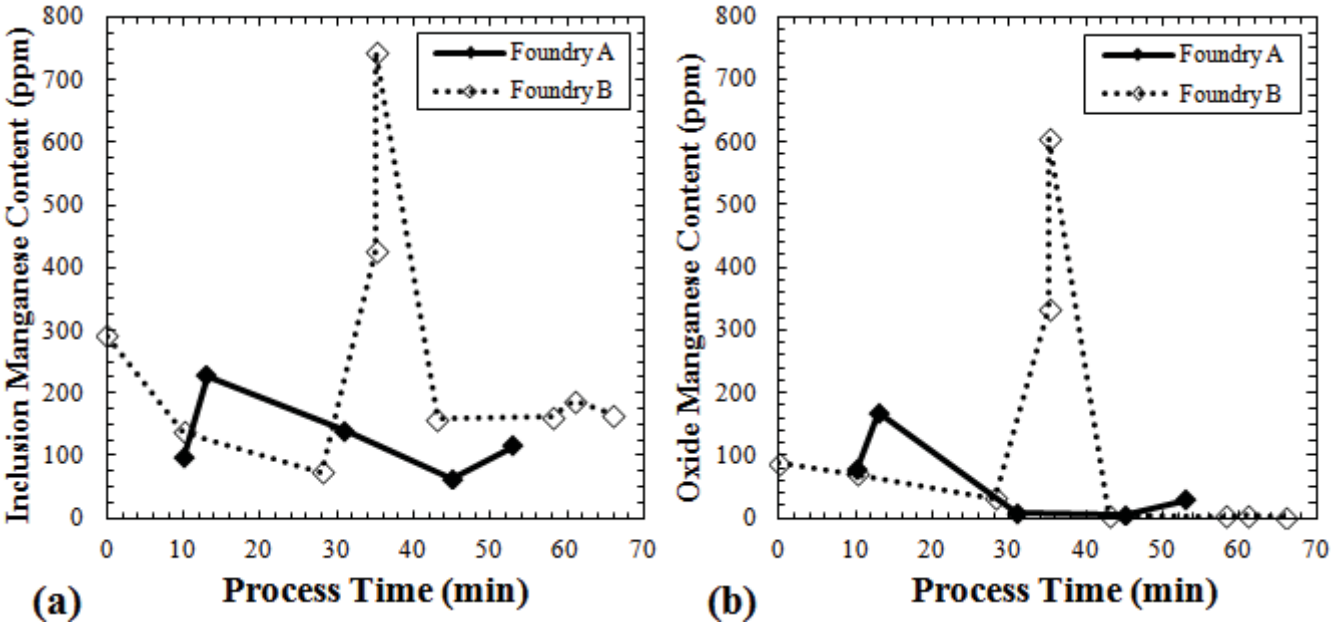

Figure 11. Manganese content within a) all inclusions scanned and b) only oxides < 30% sulfur.

Analyzed Section Area

Comparing the results for the two sectioning methods, it was found that the center sectioned immersion samples had a larger measured inclusion area fraction than the surface method (see Figure 12). This has been attributed in large part to inclusions formed at low temperatures such as manganese sulfide, which depend largely on cooling rate. The surface ground region of the immersion sample is the closest to steel chill plates resulting in much faster cooling rates compared to the central region of the sample. That is, the slower cooling rate in the center allows more time for inclusions such as manganese sulfide to form while the faster cooled surface does not. Inclusions such as manganese sulfide, which form during solidification or upon cooling, can alter primary inclusions: those that are present in the liquid steel. These primary inclusions often serve as sites for preferential nucleation which affects the measured composition and size. It is important that areas selected for analysis be representative of primary inclusions when trying to study liquid steel processing. Thus, the most representative section of the immersion sampler is the surface (fastest cooling) but is also the most prone to contamination via slag entrainment and flotation effects. In some cases center sectioning is a superior alternative, especially when contamination issues are prevalent.

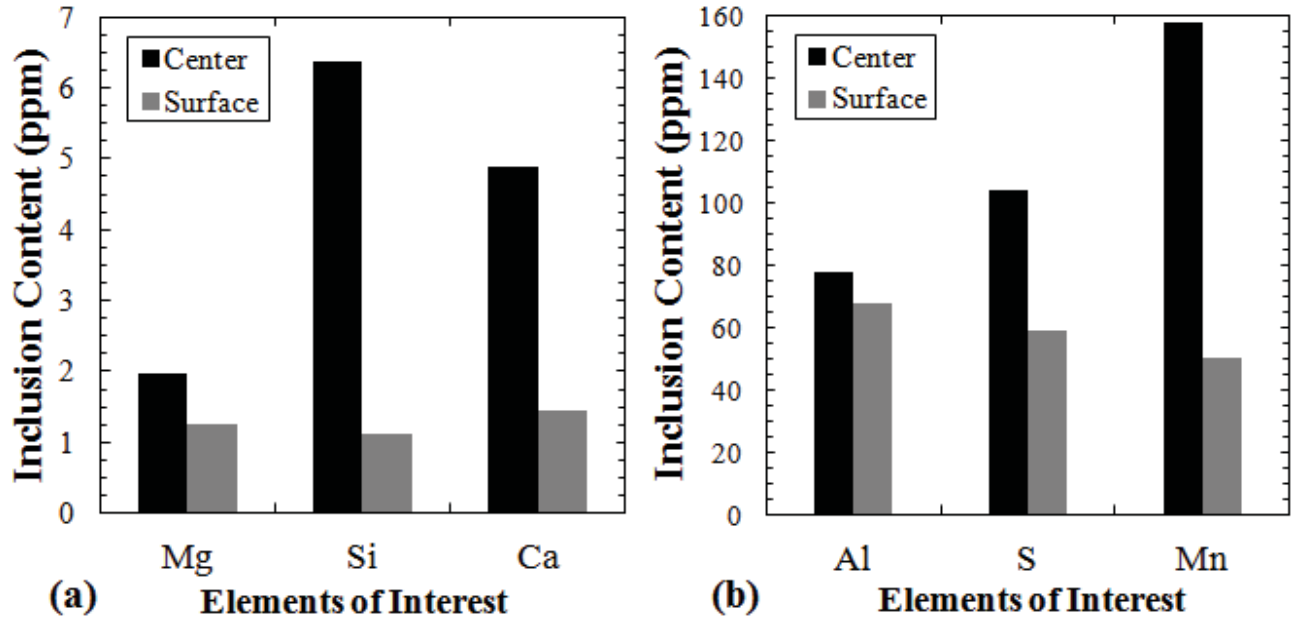

Figure 12. Elemental content within all scanned inclusions in specimens prepared by two sectioning methods: a) minor elements and b) major elements present in inclusions.

DISCUSSION

Inclusion compositions are typically represented using single ternary diagrams. The problem with this form of representation is that the inclusion populations present contain more than three elements (often 6 or 7 depending on the composition of the steel). Normalization is therefore implicit in these representations and can lead to large errors in interpretation. A system was developed for representing different inclusion classes by combining six different ternaries allowing for the representation of up to 7 elements. Each ternary represents a distinct inclusion population with each individual inclusion counted only once and shown in the respective ternary section it belongs. The technique considers the three most abundant elements of a particular inclusion in assigning ternary sections and these elements typically account for more than 80% of the inclusion composition, thus errors associated with normalization are greatly reduced. In addition to minimizing normalization errors, ternaries seldom have morphological factors such as size included which can mislead interpretation (e.g. large exogenous inclusions of differing composition). Therefore, inclusion diameter is also represented in the joint ternaries developed in this study and displayed through different colors and marker size. Figure 13 is an example of a joint ternary showing the advantage of this method of representation where different types of inclusions can be examined in a continuous plot.

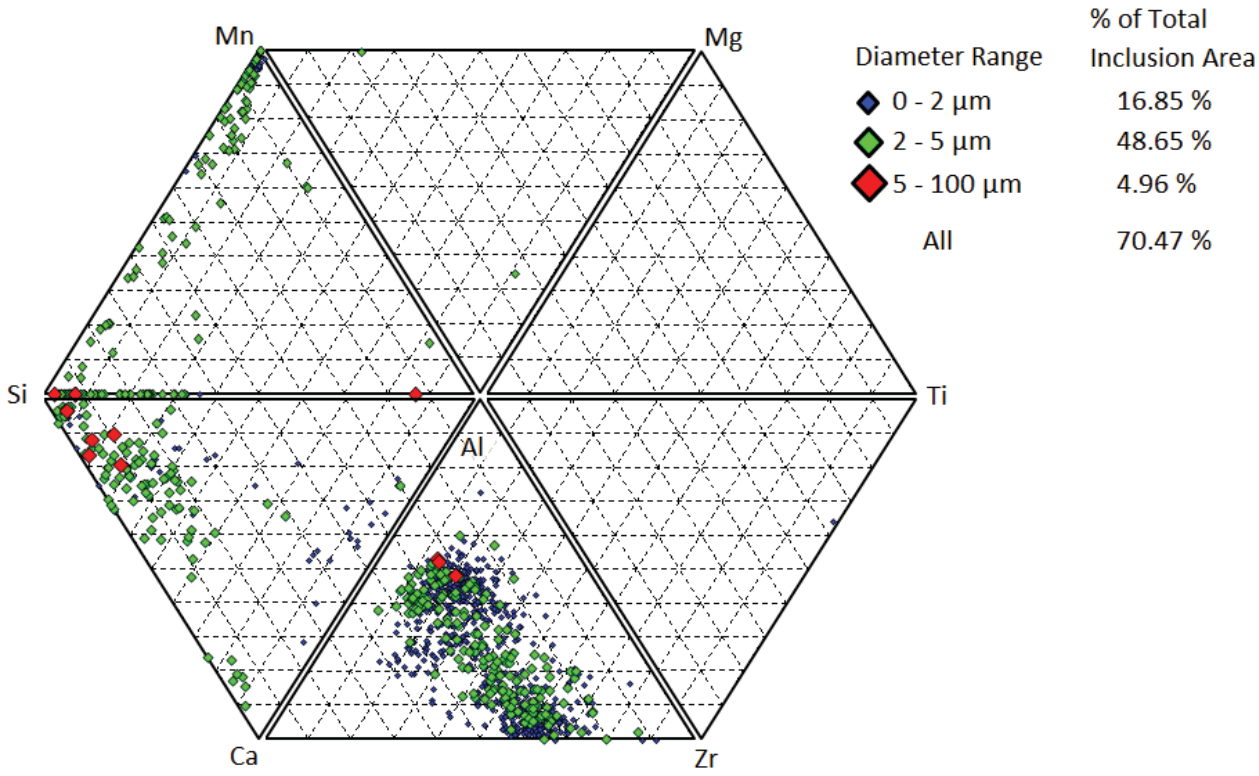

Figure 13. Joint ternary showing different classes of inclusions and their respective sizes (depicted through different colors and sizes of markers).

The evolution of inclusions throughout liquid processing has been studied for both foundry and mill samples using joint ternaries yielding a more comprehensive understanding of inclusion development. Figure 14 shows one such analysis for samples taken at different stages of LMF processing in a mini mill with the phase boundaries overlaid on the diagram. The heat studied was aluminum killed, calcium treated, and was the second heat of a four heat sequence. The ternaries shown represent samples taken after de-oxidation, before de-sulfurization, after de-sulfurization, and after calcium treatment. After de-oxidation, the inclusion population is seen to be aluminum rich (Figure 14a). With time, coarsening is observed in the aluminum oxide inclusion population (Figure 14b). After de-sulfurization there is a shift in the inclusion population towards spinel formation (Figure 14c). After calcium treatment, modification of alumina and spinel inclusions is observed as well as the formation of large calcium sulfide (CaS) population (Figure 14d).

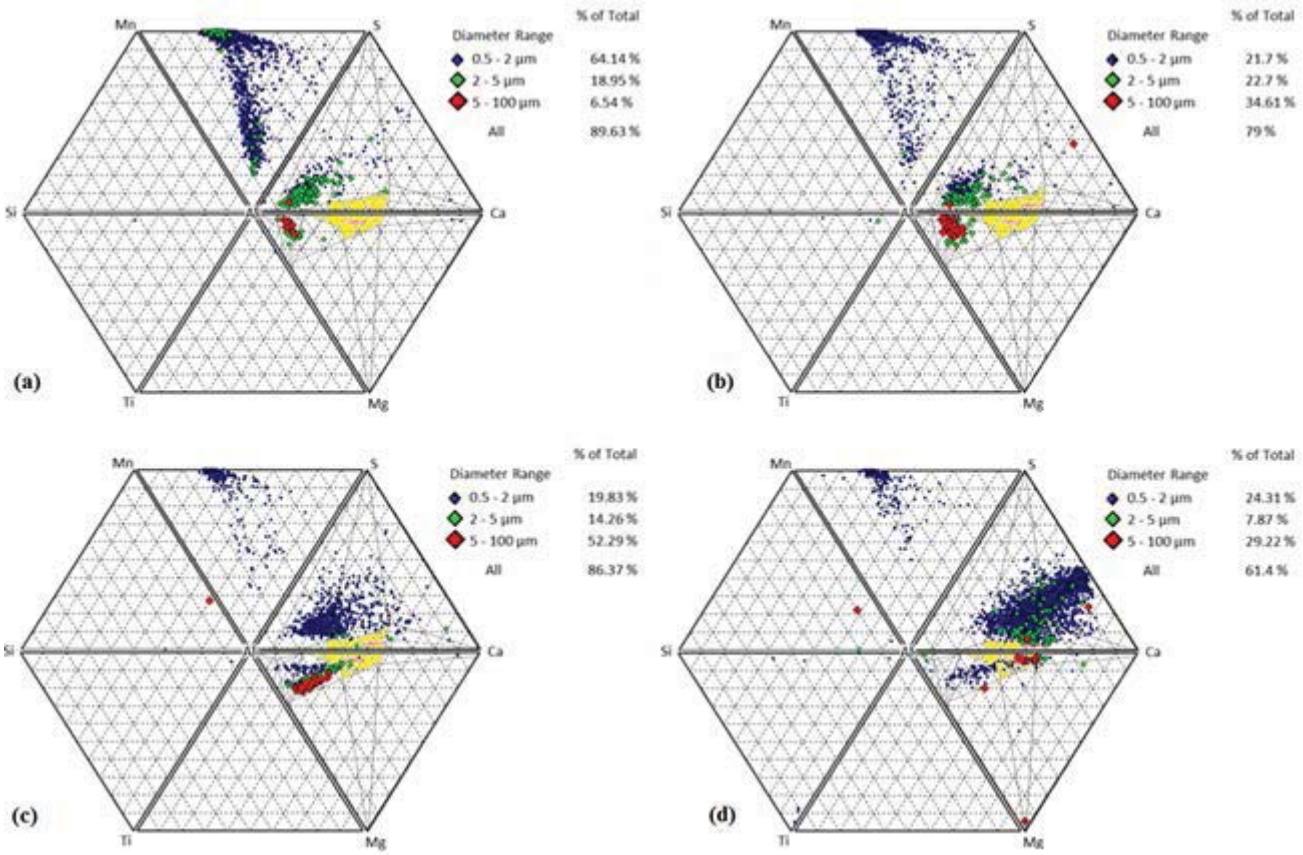

Figure 14. Joint ternaries for samples taken in a steel mini mill (a) after de-oxidation, (b) before de-sulfurization, (c) after de-sulfurization, and (d) after calcium treatment.

CONCLUSION

The effect of AFA settings; step size and magnification, on the number density and area fraction of inclusions was investigated using an automated SEM/EDS system along with sampling technique. Both the number density and area fraction increased with increasing magnification and decreased with increasing step size. The magnification was found to have a greater effect on the measured area fraction and diameter, while the step size had a more pronounced effect on the number of inclusions detected. For accurate analysis, the selected step size should be less than the minimum diameter threshold selected for inclusion analysis in accordance with Equation 3. It was also found that analysis of a rapidly cooled sample resulted in a more accurate representation of inclusion populations present in liquid steel; however the surface was found to be more likely to be contaminated with entrained slag.

New post processing methods and representation techniques for inclusion data acquired from SEM/EDS systems have been developed. These included: areal average compositions, mass balance calculations yielding the mass of an element in a sample present in the form of inclusions, and joint compositional ternaries with size data included. The mass balance correlation accuracy was measured through an oxygen result comparison with the more established inert gas fusion analysis technique and found to be largely within the 95% confidence intervals. This mass balance technique was used in the sample sectioning representativeness study. In addition to a mass balance calculation technique, a method of qualitatively displaying inclusion compositions and morphologies for highly varied inclusion populations was established as an expansion of more traditional single ternaries in the form of a joint ternary system.

REFERENCES

1. Zhang, Lifeng, and Brian Thomas. "State of the Art in the Control of Inclusions during Steel Ingot Casting." *METALLURGICAL AND MATERIALS TRANSACTIONS B* 37B.October (2006): 733-60. Print.
2. Winkler, W., J. Angeli, and M. Mayr. "Automated SEM-EDX Cleanness Analysis and Its Application in Metallurgy." *BHM* 152.1 (2007): 4-9. Print.

3. Kaushik, P., H. Pielet, and H. Yin. "Inclusion Characterisation – Tool for Measurement of Steel Cleanliness and Process Control: Part 1." *Ironmaking and Steelmaking* 36.8 (2009): 561-71. Print.
4. Kaushik, P., H. Pielet, and H. Yin. "Inclusion Characterisation – Tool for Measurement of Steel Cleanliness and Process Control: Part 2." *Ironmaking and Steelmaking* 36.8 (2009): 572-82. Print.
5. Meyer F Ruby, Evrard S. Vergauwens M., Balland P. "Improvement of the Sampling Methodology for the Cleanliness Measurement in the Liquid Steel Stage." *AISTech 2013 Proceedings* (2013): 1051-059. Print
6. Singh, Vintee, Kent Peaslee, and Simon Lekakh. "Use of Automated Inclusion Analysis to Evaluate the Effects of Ladle Treatment on Steel Cleanliness." 63rd SFSA T&O (2009): 1-15. Print.
7. Singh, Vintee, Simon Lekakh, Timothy Drake, and Kent Peaslee. "Process Design of Inclusion Modification in Cast Steel Using Automated Inclusion Analysis." *AISTech 2009 Proceedings* (2009): 1-11. Print.
8. Shi, Dexiang, and Douglas Winslow. "Accuracy of a Volume Fraction Measurement Using Areal Image Analysis." *Journal of Testing and Evaluation* (2012): 210-13. Print.
9. Ericsson, Ola. *An Experimental Study of Liquid Steel Sampling*. Thesis. Royal Institute of Technology, 2009. Print.
10. Nuspl, Markus, Wolfhard Wegscheider, Johann Angeli, Wilhelm Posch, and Michael Mayr. "Qualitative and Quantitative Determination of Micro-inclusions by Automated SEM/EDX Analysis." *Analytical and Bioanalytical Chemistry* 379 (2004): 640-45. Print.
11. Michelic, Susanne, Gerhard Wieser, and Christian Bernhard. "On the Representativeness of Automated SEM/EDS Analyses for Inclusion Characterisation with Special Regard to the Measured Sample Area." *ISIJ International* 51.5 (2011): 769-75. Print.
12. Abraham, Sunday, Justin Raines, and Rick Bodnar. "Development of an Inclusion Characterization Methodology for Improving Steel Product Cleanliness." *AISTech 2013 Proceedings* (2013): 1069-084. Print.
13. Zhang, Zhi, Anders Tilliander, Andrey Karasev, and Par Jonsson. "Simulation of the Steel Sampling Process." ISIJ International 50.12 (2010): 1746-755. Print.